PERGAMON

Building and Environment 37 (2002) 109–121

BUILDING AND ENVIRONMENT

www.elsevier.com/locate/buildenv

Study of solar walls — validating a simulation model

L. Zalewski[a,*], S. Lassue[a], B. Duthoit[a], M. Butez[b]

[a] *L.A.M.H. (Laboratoire de l'Artois de Mécanique et Habitat), Equipe Thermique et Instrumentation, Faculté des Sciences Appliquées, Technoparc Futura - 62400, Bethune, France*

[b] *C.E.A de CADARACHE. (Commissariat á l'Energie Atomique), DER/SSAE/LVT, GENEC, 13108 St Paul-lez-Durance Cedex, France*

Received 20 August 1999; received in revised form 15 November 1999; accepted 2 August 2000

Abstract

The aim of this article is to present the results of a comparative study of four different types of solar wall. These results have been obtained using a numerical simulation model. In order to validate the model, an extensive experimental study has been conducted on a composite solar wall. The first part of the article is devoted to the particular features of the four solar wall configurations, followed by a description of the experimental installation, the measurements and study of the various modes of thermal transfer necessary for the model to be validated. The third section begins with a brief presentation of the principle used to develop this model, continuing with the validation phase. The model is then used to study the energy efficiency of solar walls in different locations and under different climatic conditions. This is followed by an analysis of the way in which they release the energy supply, and their performance during the summer period. The results of this study are fundamental in helping architects or project managers to choose the best suited configuration for each type of building.

Keywords: Solar walls; Experimental study; Efficiency of solar walls

1. Introduction

There has been extensive use of solar energy for heating buildings by means of storage walls since the works of Trombe [1–5] were published. The standard Trombe wall (Fig. 2) has the drawback of low thermal resistance, which leads to significant losses at night-time or during periods with no sun. Furthermore, part of the supply stored in the mass cannot be controlled (risk of overheating in mid-season). This type of wall requires a solar shield to be fitted for the summer period in order to avoid unwanted supplies during this time. We have studied a different configuration of solar wall which enables these drawbacks to be overcome; this wall is called a composite solar wall, or a Trombe–Michel wall [6,7].

This article will present the results of a numerical simulation model developed and validated using experimental measurements conducted over three consecutive years on a prototype wall. The first section of the article covers the presentation of four different types of solar wall, the Trombe wall, the insulated Trombe wall, the non-ventilated solar wall and the composite solar wall. We shall then describe the experimental installations which enabled us to obtain the measurements and the thermal study of the composite solar wall. The following section is a description and validation of the model. Once validated, the model, associated with the technique of factorial plans, enabled us to identify the parameters which influence the efficiency of the solar wall. The last section of the article will be devoted to comparing the four different solar walls with regard to their energy efficiency (mode and time for releasing the energy collected) and with regard to the unwanted energy supplies in summertime.

2. Presentation of the different types of passive solar wall

Passive solar walls are included in the shell of a building. Their function is to enable solar energy collection in order to reduce the quantity of paying energy consumed for standard heating installations. This "free" energy supply differs from direct solar gains obtained through glazed surfaces due to the use of a storage wall. This wall, as its

* Corresponding author. Tel.: +33-3-2163-7153; fax: +33-3-2163-7123.

E-mail address: laurent.zalewski@univ-artois.fr (L. Zalewski).

0360-1323/02/$ - see front matter
PII: S0360-1323(00)00072-X

Nomenclature

$\dot{m}$	mass flow (kg s^{-1})
P_{enth}	power provided to the air in the ventilated air layer (W)
S_{exch}	exchange surface (m^2)
T_{cv}	surface temperature of the wall measured using the thermocouple inserted at the convective fluxmeters (°C)
T_s	surface temperature of the storage wall (°C)
T_a	air temperature measured inside the air layer (°C)
T_{Sext}	wall surface temperature on the external side (°C)
$T_{ins.LA}$	insulation surface temperature on the air layer side (°C)
$T_{ins.room}$	insulation surface temperature on the room side (°C)
T_{uv}	air temperature at upper vent (°C)
T_{Lv}	air temperature at lower vent (°C)

Indices

U	Measurement at the upper part of the air layer
M	Measurement mid-way up the air layer
B	Measurement at the bottom part of the air layer

Greek letters

ρ	density of fluid (kg m^{-3})
ϕ_{cv}	density of convective flux measured in the ventilated air layer (W m^{-2})
ϕ_{glob}	density of global flux (convective + radiative) measured in the air layer (W m^{-2})
ϕ_{ext}	density of flux measured on the external side of the wall (W m^{-2})

name suggests, stores heat during the sunny periods and releases it with a time lag which depends on the characteristics of the wall. This supply can be used in addition to direct solar gains, and thereby limit the risks of overheating.

Over time, modifications have been made to solar walls in order to improve their efficiency.

Four different configurations of solar wall are presented below, with their main advantages and disadvantages.

The composite solar wall (Fig. 1) comprises a transparent outer cover, an enclosed air layer, a storage wall, a ventilated air layer, and finally an insulation layer in which two vents have been drilled. It works as follows. The storage wall absorbs part of the solar energy and heats up by greenhouse effect, stores and transmits the energy by conduction towards the inside of the building. After a certain time lag, depending on the type and thickness of the wall, part of this energy is exchanged by convection with the air, the rest being exchanged by radiation with the insulation layer. A very small part of this energy received by radiation is transmitted by conduction towards the inside of the building, the rest is transferred to the air by convection. Therefore, nearly all the supply is provided to the building by means of the ventilated air layer. By blocking off the circulation of the air, the supply is also stopped, thereby avoiding any overheating, or the problem of reverse heat circulation.

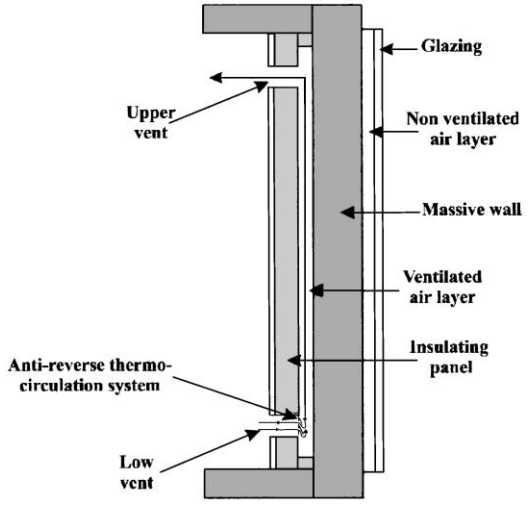

Fig. 1. Composite solar wall.

The composite solar wall has the following advantages:

- Good heat resistance (due to the presence of the insulation layer and the air layers).
- No infiltration of cool air through the outside cover.
- Due to the existence of the insulation layer, the supply in summertime is limited. This is done by blocking off the air circulation in the ventilated layer and, if possible, opening the outside air layer.
- The supply stored in the mass is released by means of the ventilated layer, after a length of time which depends on the type and the thickness of the wall.
- The supply can be controlled at all times by adjusting the air circulation.

Its main drawback is that it requires a system to prevent reverse heat circulation in the ventilated air layer. This problem arises when the storage wall is colder than the air in the ventilated layer. In that case, unless a system is provided to block off the circulation, the air is cooled and re-injected into the room through the lower vent. This statement is also true for the standard Trombe wall, shown in Fig. 2, the configuration which was to lead to the development of the composite solar wall.

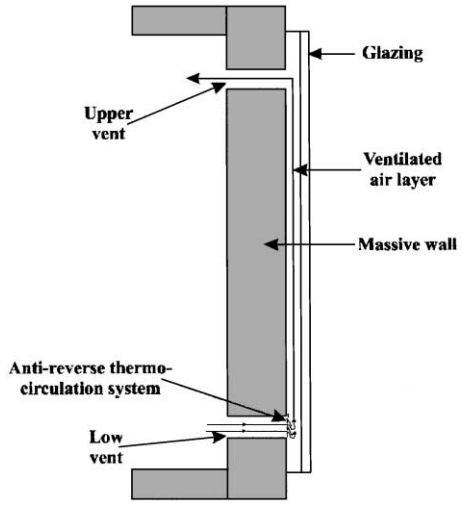

Fig. 2. Trombe wall.

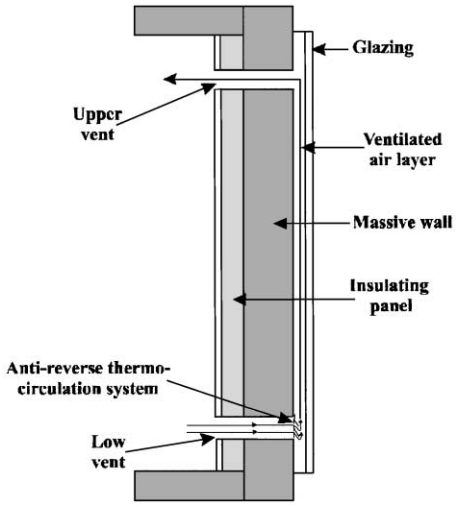

Fig. 3. Insulated Trombe wall.

By heating the air in the outside ventilated air layer by convection, the supply is quickly released into the room, whilst maintaining the advantages of storage in the mass. This configuration has the advantage of being more efficient as compared to the previous one. A major drawback, apart from the problem of reverse heat circulation, is the lack of control over the energy supply (convection and radiation) by the storage wall. Furthermore, supplies from the ventilated layer are virtually direct solar supplies (risk of overheating). It should be noted that this configuration requires the transparent cover to be perfectly airtight in order to avoid any likelihood of infiltration of cold air. This configuration requires a solar shield to be fitted in order to reduce unwanted energy supplies during summertime.

To increase the thermal resistance of the Trombe wall and control supplies, it is possible to fit an insulation layer on its back (Fig. 3). The advantage of this insulation layer is that it improves the thermal resistance of the Trombe wall, and therefore offers the possibility of controlling supplies by simply adjusting the air circulation. Moreover, this insulation layer blocks off virtually all the supply in summertime. It is therefore no longer essential to fit a solar shield. However, the presence of the insulation limits supply for the storage mass; virtually all the energy collected is therefore rapidly directed into the room by the air layer (short time lag).

We must not forget that this configuration, like the previous one, requires the transparent cover to be perfectly airtight.

The fourth and last configuration is the simplest and the oldest configuration. In this case, the wall (Fig. 4) comprises a transparent cover, an enclosed air layer and a storage wall. It works as follows: the storage wall absorbs the solar energy, and heats up by greenhouse effect, stores the energy and transmits it by conduction inside the room.

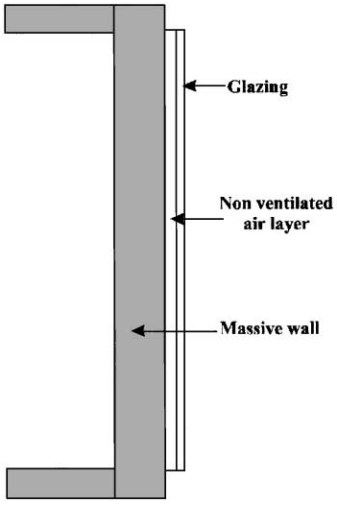

Fig. 4. Non-ventilated solar wall.

The energy is then released into the room by convection and radiation. The main advantage of this configuration is its simplicity.

Its disadvantages are a lack of control in the supplies stored in the mass, poor global thermal resistance of the wall (extensive losses at night and during periods with no sun) and the necessity of a solar shield in summertime to avoid unwanted energy supplies.

After presenting several solar wall configurations, we are now going to present the experimental composite solar wall which has been used first for conducting a thermal study of the wall.

We have just presented the various types of passive solar walls, with their main advantages and disadvantages and operating principles. They use the different heat transfer modes that can usually be found in buildings simultaneously. To study and compare the efficiency of these

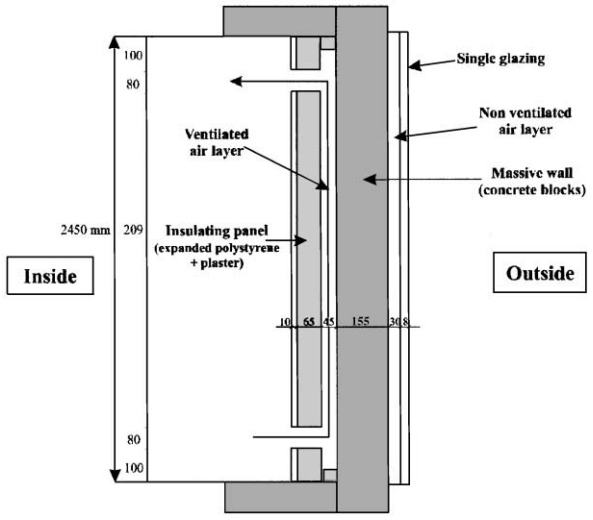

Fig. 5. Vertical cross-section of experimental composite solar wall.

walls, it is essential to conduct very detailed research into the various physical phenomena involved in collecting and transferring heat from outside into the premises that are to be heated. Extensive research has been conducted on this subject and is summarised as follows.

3. Experimental study

3.1. Experimental composite solar wall (geometry and composition)

An experimental wall (Figs. 5 and 6) was built as similar as possible to those built using normal civil engineering practices. Hollow breeze-blocks 20 cm thick, solid breeze-blocks and an air layer 5 cm thick were used to obtain continuity over the two sides of the wall. To limit the losses through the sides by conduction, a thin layer of insulation was fitted (see Fig. 6).

3.2. Experimental facility

The experimental composite solar wall was built on the south side of a test cell under real conditions at the test facility of Atomic Energy Centre (CEA) at Cadarache (latitude: 43° 39′ 18″ N; longitude: 5° 46′ 21″ E; altitude: 268 m). It was studied over a period of nearly three years [8], using a full range of instrumentation. This instrumentation included thermocouples, tangent gradient fluxmeters [9], two hot-wire anemometers, environmental temperature probes (convective temperature and dry resultant probes) and measurement sensors for meteorological parameters (solar flux density on a vertical wall, wind speed and outside temperature). Figs. 7 and 8 show the position of the measurement probes and the list of variables.

The signals measured using these sensors were used for validating a thermal simulation model that was developed at the same time. The tangent gradient fluxmeters, in this case, have virtually no perturbing effects on the flux to be measured [10]. Two series of 3 fluxmeters, 15×15 cm^2 in size, were fitted symmetrically in the ventilated air layer on the concrete wall (see Figs. 7 and 8). These sensors also include integrated "T"-type thermocouples enabling simultaneous measurement of the heat flux density and temperature. One series of fluxmeters was covered with a slightly emittent coating layer (polished aluminium $\varepsilon = 0.05$). The heat flux density measured was therefore essentially convective (ϕ_{cv}) [11–13]. The other series of sensors was covered with a coating layer of the same emittance as the wall to provide data concerning the global heat flux density (ϕ_{glob}) exchanged (convective + radiative) by the storage wall. Measurements of temperatures (T) and speed (hot-wire anemometer) in the ventilated air layer completed the arrangement.

Before passing on to the model validation phase, the model must include geometric characteristics, the thermophysical characteristics of the various elements of the wall, the correlation adapted for calculating the exchange coefficients, etc.

To compile this database, several studies have been conducted, based on the various experimental measurements. The purpose of these studies and the various results obtained are summarised in the following section.

3.3. Experimental studies

Firstly, we examine the storage wall; by means of simultaneous measurements of flux and temperature on the two sides of the massive wall, it was possible to establish the thermo-physical properties (thermal conductivity, product ρC) [14,15]. Conductivity and thermal capacity of the insulation layer were measured in the laboratory using a method also based on flux measurements [16]. The air circulating in the ventilated layer collects heat from the storage wall by convection, and from the insulation layer before releasing it to the room building. The flux density meters placed on the massive wall were the essential elements for the study of superficial exchange within the ventilated air layer. The measurements of convective flux density enabled in-situ calculation of the coefficients of exchange by convection, and also selection of a correlation adapted to the composite solar wall [13]. This was then integrated into the model. Based on this principle, an original method for energy balance of the air layer was produced. This method has been compared with other more standard "processes" (enthalpy balance, or calculation of load losses) [12,14].

Measurements of global flux density (convection+ radiation) enabled the respective shares of flux density exchanged by convection and radiation to be estimated [11,12].

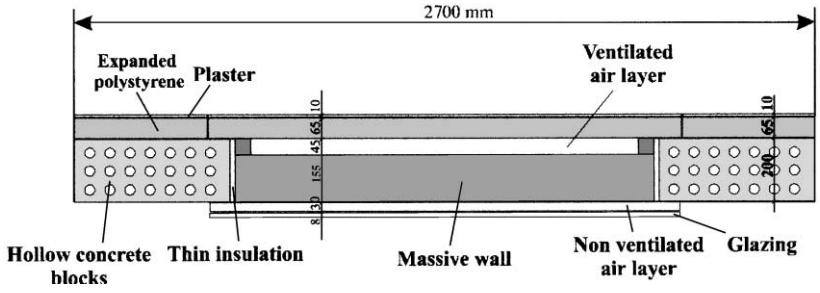

Fig. 6. Horizontal cross-section of the composite solar wall.

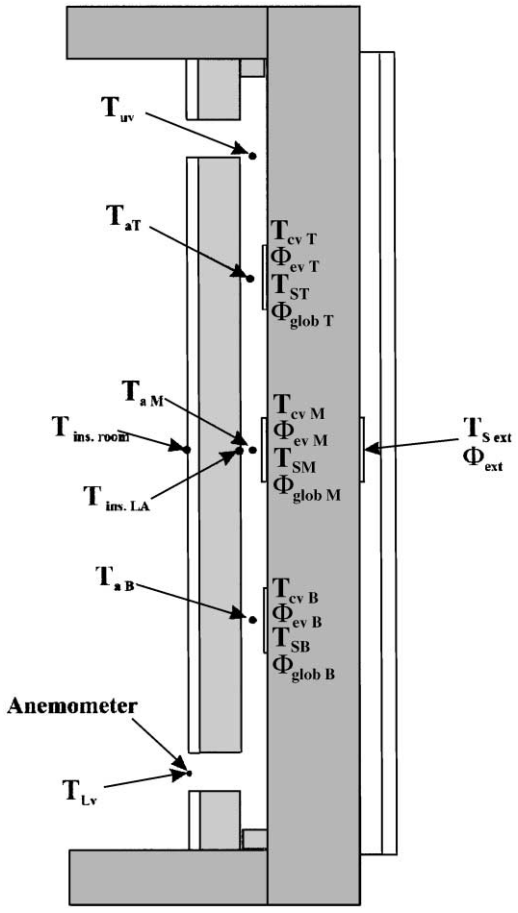

Fig. 7. Instrumentation — vertical cross-section.

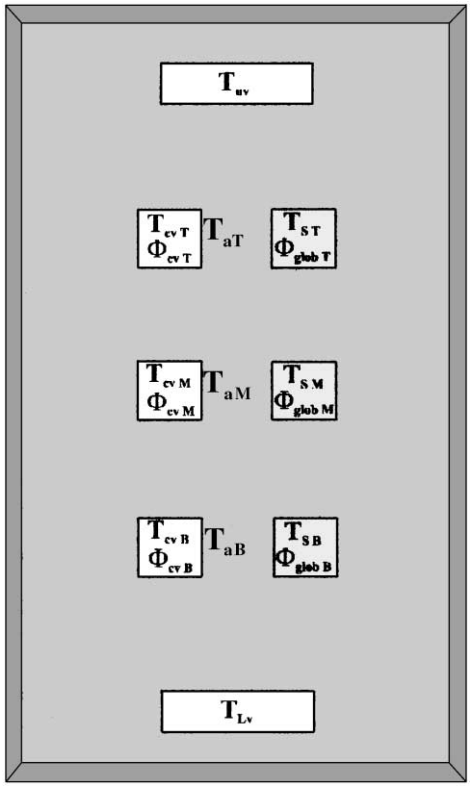

Fig. 8. Instrumentation — front view.

The results obtained during these experimental studies contributed in gaining a better knowledge of the thermophysical properties of the different elements of the wall. All these extremely precious data have been used in validating the model. This phase has been extensively described elsewhere [8,13] and will not be explained here.

4. Modelling — validation

4.1. Description of the model

A model for thermal calculation [8], based on the finite difference method, enables simulation of the temperature range within a wall placed between two environments, in a variable system and in one dimension. The wall is divided into meshes, at which the thermal balance is assessed. Each wall comprises different media (solid, enclosed air layer, or ventilated air layer), divided into mesh sections of identical size, with node points at the intersections. The nodes placed at the limits are included in the balance of solid–air exchanges. The heat transfer is considered to be one dimensional, heat losses through the surfaces at the sides are therefore negligible. To compute the temperature field in the wall, it is necessary to solve a system of equations of balances established at the various node points. An iterative process is used to compute the solution, assuming a linearised system at each iteration, and checking that the assumed initial and final temperature fields are consistent. The simplifications used have

an influence on the accuracy of the model, so a validation phase is essential.

4.2. Validating the model

In order to validate the model, experimental data are compared with simulated data. These data concern physical magnitudes (temperature, flux density) which are representative of how the composite solar wall works. The data of interest are, therefore, the internal and external surface temperatures of the storage wall, the flux densities exchanged on the previously mentioned surfaces, and finally the power collected by means of the ventilated layer. Fig. 9 shows the evolution of climatic conditions (solar flux density (global vertical) and outside temperature). For the sake of clarity, the sequence presented has been limited to 4 days. For this test, the configuration of the composite solar wall is as follows:

- Outside cover: single glazing (8 mm).
- Thickness of the enclosed air layer 3 cm.
- Colour of the outside surface: black.
- Thickness of the storage wall: solid concrete blocks of 15 cm.
- Ventilated air layer thickness: 4.5 cm.
- Insulating wall: 7.5 cm of polystyrene + 1 cm of plaster.
- Size of vents: 60×15 cm^2.
- The surface of the wall is 3.3 m^2.
- The reverse heat circulation protection system is a motorised opening, controlled by a fluxmeter [8,13].

Fig. 10 shows the flux densities measured and calculated on the outside surface ($\phi_{ex}t$) and the convective flux densities measured and calculated on the inside surface of the storage wall.

Fig. 11 shows the temperatures measured and calculated over the same surfaces of the storage wall.

Fig. 12 shows the power collected by means of the air layer.

P_{calc} is the power collected calculated by model.

P_{enth} is the experimental power obtained from a measurement of mean air flowrate at the lower vent, measurements of air input and output temperatures: $P_{enth.} = \overset{\circ}{m}\ C_p[T_{uv} - T_{Lv}]$. P_{flux} is the experimental power deduced from the heat fluxmeter measurements: $P_{flux} = [\phi_{cv.massive\ wall} + \phi_{cv.insulation}] \times S_{exchange}$ [12,14].

Figs. 10–12 demonstrate that there is good correlation between the measured data and the simulated data. The deviation between temperatures or flux densities is lower than 5% and the maximum deviation between the different powers is less than 10%. Similar comparisons have been made over several periods of time, and have led us to prove the reliability of our model [8,17]. Several different composite solar wall configurations have been studied for this reason over long periods of time; modification to the solar absorption coefficient of the storage wall, replacement of the outside cover, modification in the thickness of the insulation layer, modification in the size of the vents, in the thickness of the enclosed air layer, etc. The model has, therefore, become an indispensable tool for the next part of our work.

4.3. Advantages of the model

The advantage of the model (thus now validated) lies in the possibility of modifying a certain number of parameters and obtaining results very quickly. This enables the study of typical cases to be conducted [8].

Using the method of factorial plans, we can identify the essential parameters to have an influence on energy efficiency of the composite solar wall. Furthermore, it is also possible to study the time necessary for release of the energy collected by the composite solar wall, its level of efficiency depending on the thickness of the wall. It is also of interest to be aware of the effect on efficiency of solar walls made of different elements, the direction they face and their site of installation.

The supply in summertime, which is one of the major problems with solar walls, can be quantified. It is also possible to compare the operation and the efficiency of different types of solar wall (unventilated wall, Trombe wall, insulated Trombe wall, composite solar wall). We suggest that we examine these two last points in the coming section.

5. Simulation

5.1. Level factorial plan

The factorial plan technique [19,20] is a technique to assess the influence of different parameters (or variables) on a given phenomenon. This is done by expressing the phenomenon in the form of a simple equation which is dependent on the different parameters. Before reaching this equation, we should specify what is meant by *factorial plan* and *level.*

- The *levels* of a variable represent the whole set of possible values for the variable.
- A *factorial plan* is an experimental plan within which each level of each of the parameters is associated once with each level of the other factors.

Therefore, in two-level factorial plans, each production of such a plan requires conducting $n_{exp}\,2^n$ experiments, where n is the number of parameters the effects of which we wish to measure, and n_{exp} the number of experiments conducted for each of the 2^n experimental conditions.

However, for us, the results of the experiments are obtained from simulation (n_{exp} will, therefore, always be

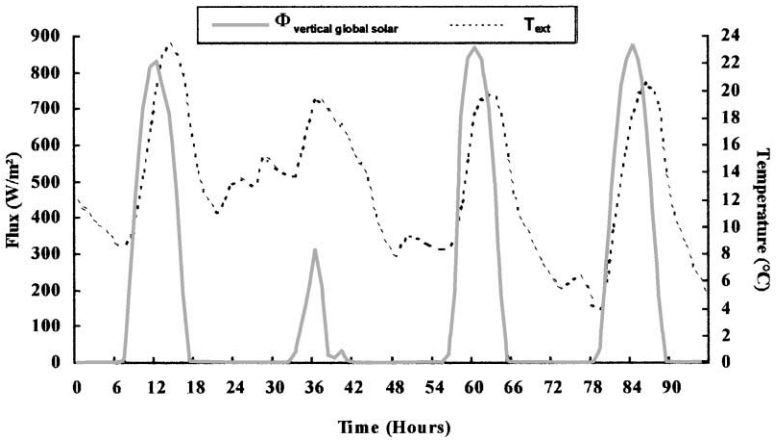

Fig. 9. Meteorological data.

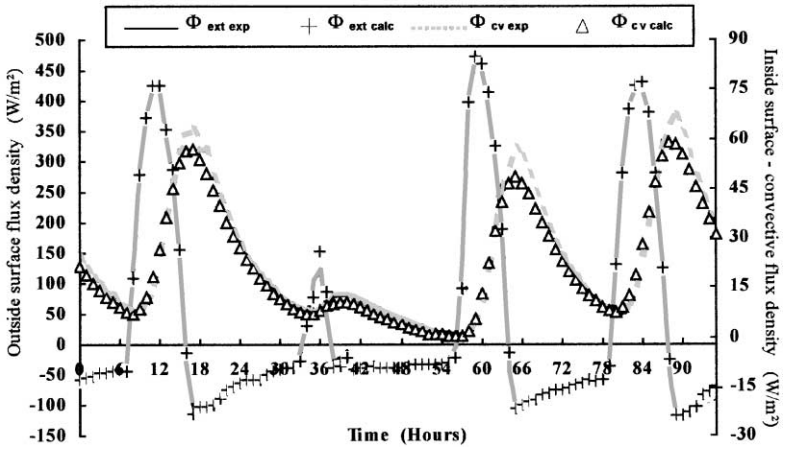

Fig. 10. Flux denisites exchanged over the two surfaces of the storage wall.

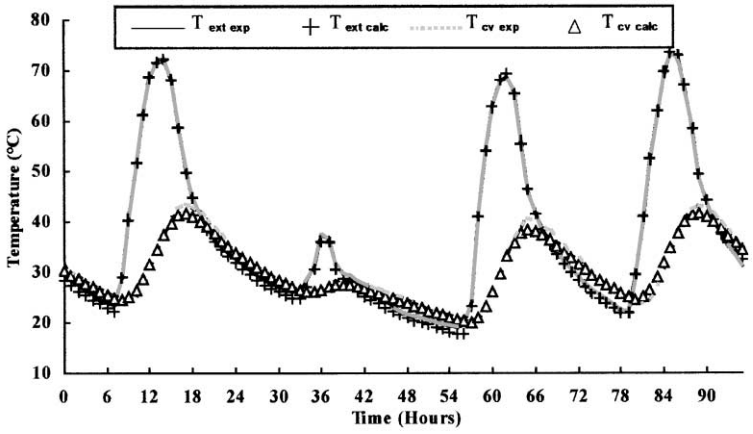

Fig. 11. Temperatures of the two sides of the storage wall.

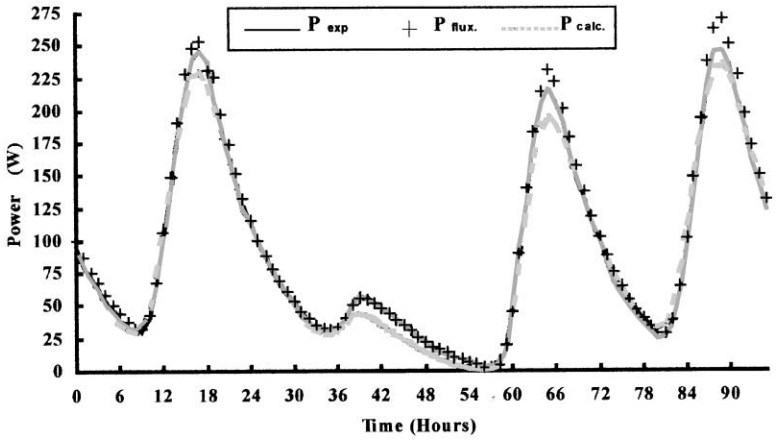

Fig. 12. Power supplied to the premises.

equal to 1 since the computer will always give the same result for each of the simulations).

The advantage of experiment plans is that they offer the possibility of exploring a region of parameter space and can show dominant trends in order to direct ulterior experimentation. However, the disadvantage of such plans is that they double the number of experiments when a new parameter is introduced.

The nature of the variables taken into consideration can be either quantitative or qualitative. The encoding of the variables is done so that for the quantitative variables, the minus sign represents the low level and the plus sign the high level. For qualitative variables, the two levels can be encoded by either a minus sign or a plus sign (it is nevertheless preferable to keep a logical notation).

To demonstrate the advantages of this technique, we have taken the example of a composite solar wall with a configuration similar to that of our experimental wall. Three parameters are tested (X_1, X_2, X_3). In this two-level factorial plan, two parameters are quantitative (the thickness of the wall and the solar absorption coefficient of the outside surface of the storage wall), and one is qualitative (the type of glazing).

The result of the experiments (here, numerical simulations) corresponds to the energy provided to the building by means of the composite south-facing solar wall for 1 m^2 of collector located in Carpentras.

The objective now is to carry out calculations for each possible combination (i.e. $2^3 = 8$ calculations) (Tables 1–3).

After obtaining the eight results, the aim now is to assess the effect that each parameter produces on the energy collected.

5.1.1. Measuring the main effects

Definition: the effect of each of the factors can be considered as the difference between two averages. Main

Table 1
Presentation of parameters

Parameters	Designation	Minimum value: −1	Maximum value: +1
Thickness of the storage wall	X_1	10 cm	15 cm
Absorption coefficient (α)	X_2	0.8	0.9
Type of glazing	X_3	Single glazing (SG)	Double glazing (DG) with low emittance

Table 2
Table showing the variables in their original units

Result number	Thickness of the wall (cm)	α	Type of glazing
1	10	0.8	SG
2	15	0.8	SG
3	10	0.9	SG
4	15	0.9	SG
5	10	0.8	DG
6	15	0.8	DG
7	10	0.9	DG
8	15	0.9	DG

Table 3
Table with encoded variables

$N°$	Thickness of the wall	α	Type of glazing (kW h m^{-2})	Energy collected
1	−1	−1	−1	$Y_1 = 69.7$
2	+1	−1	−1	$Y_2 = 58.1$
3	−1	+1	−1	$Y_3 = 85.4$
4	+1	+1	−1	$Y_4 = 72.1$
5	−1	−1	+1	$Y_5 = 177.3$
6	+1	−1	+1	$Y_6 = 166.5$
7	−1	+1	+1	$Y_7 = 202.8$
8	+1	+1	+1	$Y_8 = 190.4$

effect $= Y_{m+} - Y_{m-}$, where Y_{m+} is the mean value of responses obtained when the variable has its $+1$ level and Y_{m-} is the mean value of responses obtained when the variable has its -1 level.

For example, the main effect of the thickness of the storage wall is given by

$$\begin{aligned}\mathrm{Coef}_1 &= \frac{(Y_2+Y_4+Y_6+Y_8)}{4} - \frac{(Y_1+Y_3+Y_5+Y_7)}{4}\\ &= \frac{(58.1+72.1+166.5+190.4)}{4}\\ &\quad - \frac{(69.7+85.4+177.3+202.8)}{4}\\ &= -12.0.\end{aligned}$$

Using the same principle, it is possible to assess the main effect of α (coef_2), and the main effect of the type of glazing (coef_3).

The parameters do not necessarily behave in an additive manner, so there are interactions between parameters.

5.1.2. Measuring the interaction

Two-factor interaction: The interaction is measured by the difference between the average effect of the first parameter and the average effect of the second parameter. The semi-difference is usually known as "interaction".

$\mathrm{Coef}_{1,2}$ is the interaction of the coefficient α and the thickness of the storage wall.

α	Mean effect of the thickness of the storage wall
0.9 (+1)	$\frac{(Y_4-Y_3+Y_8-Y_7)}{4}$ ①
0.8 (−1)	$\frac{(Y_2-Y_1+Y_6-Y_5)}{4}$ ②
	Interaction $\mathrm{coef}_{1,2} = (① - ②)/2 = -0.4$

$\mathrm{Coef}_{1,3}$ is the interaction of the type of glazing with the thickness of the storage wall.

$\mathrm{Coef}_{2,3}$ is the interaction of the type of glazing with α.

Three-factor interaction:

$$\mathrm{Coef}_{1,2,3} = \frac{(Y_2 - Y_3 + Y_5 + Y_8)}{4} - \frac{(Y_1+Y_4+Y_6+Y_7)}{4}.$$

The energy collected by the composite solar wall can be expressed as follows:

$$\begin{aligned}E(\mathrm{kWh\ m^{-2}}) = \bar{X} &+ \frac{\mathrm{Coef}_1}{2}X_1 + \frac{\mathrm{Coef}_2}{2}X_2 + \frac{\mathrm{Coef}_{13}}{2}X_3\\ &+ \mathrm{Coef}_{1,2}X_1X_2 + \mathrm{Coef}_{1,3}X_1X_3\\ &+ \mathrm{Coef}_{2,3}X_2X_3 + \frac{\mathrm{Coef}_{1,2,3}}{2}X_1X_2X_3\end{aligned}$$

where $\bar{X}$ is the arithmetical mean of the eight calculated energies, X the parameter considered having as value $+1$ or -1, Coef_x the main effect of the parameter X on energy collected, Coef_{xy} the interaction of parameter X with parameter Y and Coef_{xyz} the interaction of the three parameters.

Table 4
Measuring the effects

$\bar{X}$	127.8
Coef_1	−12.0
Coef_2	19.8
Coef_3	113.0
$\mathrm{Coef}_{1,2}$	−0.4
$\mathrm{Coef}_{1,3}$	0.2
$\mathrm{Coef}_{2,3}$	2.5
$\mathrm{Coef}_{1,2,3}$	0.04

The coefficients are divided by 2 as the range of variation of variables X varies from -1 to $+1$ (the coefficients of two-factor interactions ($\mathrm{coef}_{12}, \mathrm{coef}_{13}, \mathrm{coef}_{23}$) are not divided by 2 since this coefficient is taken into account in the definition of the interaction).

The calculation of the different effects are given in Table 4

Fig. 13 enables a visual examination of the various coefficients (excepting the average $\bar{X}$).

Fig. 13 shows the importance of the various parameters. When the thickness of the storage wall is increased, the efficiency of the composite solar wall is reduced (coef_1 is negative). However, modification to the absorption coefficient (from 0.8 to 0.9) has a beneficial effect on efficiency (coef_2 equal to +19.8). Replacement of the outside cover (from single glazing to low emittance double glazing) has an even *greater effect* on efficiency (coef_3 equal to +113). It can also be considered that there is no interaction between the parameters since $\mathrm{coef}_{1,2}$, $\mathrm{coef}_{1,3}$, $\mathrm{coef}_{2,3}$, $\mathrm{coef}_{1,2,3}$. are small.

To conclude, the results of this factorial plan show that, in order to improve the efficiency of the composite solar wall, the thickness of the storage wall should not be increased too much, but the absorption coefficient of the storage wall should be improved, and above all, the losses should be limited (by reducing, for instance, the flux density of the outside part of the wall).

Other factorial plans have been made. These have shown that parameters such as the thickness of the insulating wall and the size of the vents do not have a significant effect on the efficiency of the composite solar wall.

5.2. Study of solar walls

The previous section showed that certain parameters such as the type of outside cover, the emissivity coefficient of the outside surface of the storage wall, or the absorption coefficient of the storage wall are essential in improving the efficiency of the system. To study the different configurations of solar walls, we have taken these

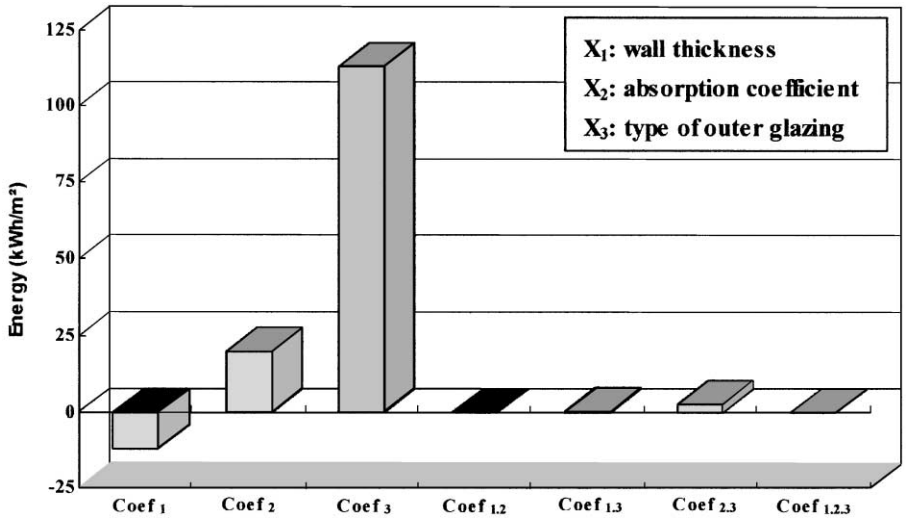

Fig. 13. Representation of the different coefficients.

aspects into account, whilst keeping the materials identical to those used for the experimental composite solar wall:

- Storage wall: solid breeze-blocks 15 cm thick.
- Enclosed air layer (thickness: 3 cm).
- Ventilated air layer (thickness: 5 cm).
- Insulating wall: 6.5 cm of expanded polystyrene + 1 cm of plaster.
- Vents: 114×7 cm^2.
- Solar absorption coefficient of the storage wall on the outside surface: 0.9.
- Transparent cover: double glazing with low emitting coating on one side ($\varepsilon = 0.15$).
- Reverse heat circulation protection system: soft plastic film or motorised opening, controlled by a flux density meter [8].

5.2.1. The efficiency of solar walls

5.2.1.1. The efficiency of solar walls with low emittance double glazing. The efficiency of a solar wall depends on the place where it is built and the direction it faces. For our calculations, the walls are considered to face south, the chosen sites are Trappes (longitude: 2°01′, latitude: 48°46′) and Carpentras [longitude: 5°03′, latitude: 44°08′).

The heating season lasts 241 days at Trappes and 196 days in Carpentras; the sum of solar energy over a vertical surface facing south is equal to 429 kWh m^{-2} in Trappes and 554 kWh m^{-2} in Carpentras. Fig. 14 represents the quantity of energy collected per m^2 of wall in Trappes or in Carpentras for each of the configurations. The energy balance for a standard insulated wall ($K_{tot} = 0.47$ W m^{-2} °C^{-1}) is also given, for reference.

Globally speaking, these results show the advantages of solar walls as compared to normal walls. If we examine the site of Carpentras, the energy gain over one heating season is $217 + 23 = 240$ kWh m^{-2} for the unventilated solar wall, 286 kWh m^{-2} for the Trombe wall, 264 kWh m^{-2} for the insulated Trombe wall and 212 kWh m^{-2} for the composite solar wall. These results also show that the most efficient solar wall is the Trombe wall and the least efficient is the composite solar wall (remember, for the composite solar wall, the supply can be controlled at all times by adjusting the air circulation).

Another essential aspect to be taken into consideration is the way in which the energy is released into the building.

5.2.1.2. The efficiency of solar walls with standard double glazing. In this section, we intend to show the huge difference between a solar wall equipped with a standard double glazing and a solar wall equipped with a low emittance double glazing.

A comparison of Figs. 14 with 15 shows the interest of the new materials or the new technologies. They are certainly important as regards the development and the implementation of solar walls which should be used more often in the future.

5.2.2. Modes and time for releasing energy supplies

Supply by convection (controllable), i.e. released by the air layer, is differentiated from supply by conduction (energy which cannot be controlled, stored in the mass, then transmitted to the premises by convective and radiative exchange on the inside surface of the solar wall). To calculate the time lag, the signals considered are the solar flux densities and the convective flux densities exchanged in the ventilated layer or on the inside surface of the solar wall. We should also specify that these times depend on the nature and the geometry of the various elements of

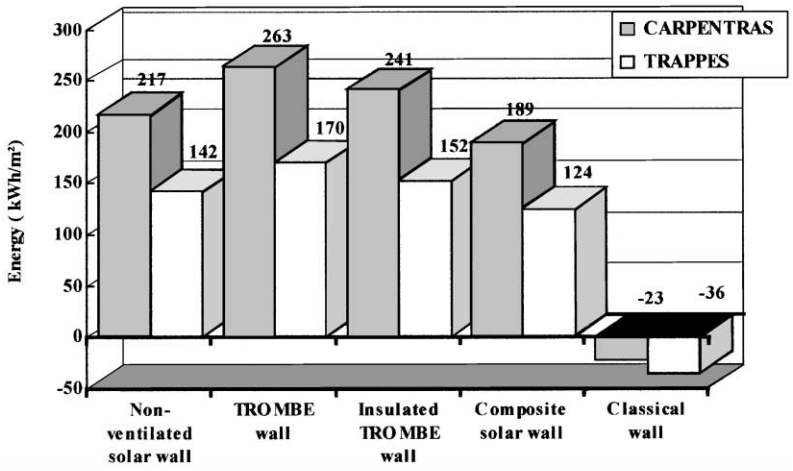

Fig. 14. Energy collected during a heating season per m^2 of wall surface (low emittance double glazing).

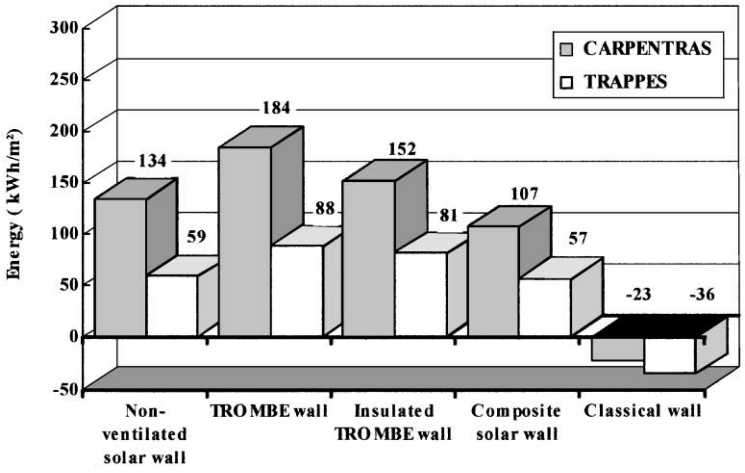

Fig. 15. Energy collected during a heating season per m^2 of wall surface (standard wall).

the solar wall. In this case, they mainly depend on the storage wall (solid breeze-blocks 15 cm thick, and with a heat conductivity equal to 0.82 W m^{-1} $°C^{-1}$). The calculations have been refined using intercorrelation functions [18].

Fig. 16 shows the importance (in %) of each releasing mode, for the various configurations. The figures at the top of each bar of the chart indicate the release time for each mode.

This figure clearly shows the advantages of the composite solar wall. For a thickness of 15 cm, this wall releases the maximum of controllable energy at the beginning of the evening (towards 6 p.m.), when direct solar gains have disappeared. Furthermore, it should be noted that more than 90% of supplies are controllable (release by air circulation). These two effects mean that it is possible to avoid the risks of overheating, therefore, periods of time when the temperature is uncomfortable.

5.2.3. Supply in summertime

The evaluation of the quantity of energy transmitted into the associated building, outside of the heating periods, was conducted considering that there was an indoor temperature of 21°C. The ventilated air layers of the Trombe, insulated Trombe and the composite solar wall were closed.

If no solar protection is provided, for Carpentras site, the unventilated and the Trombe solar walls provide 253 kWh m^{-2}; the insulated Trombe wall: 98 kWh m^{-2}; the composite solar wall: 92 kWh m^{-2}.

In Trappes, the quantity of energy transmitted to the building is the equivalent of 154 kWh m^{-2} for the unventilated and Trombe wall configurations, and approximately 60 kWh m^{-2} for the insulated Trombe and composite solar walls.

These results show that fitting insulation on the inside surface of solar walls enables the unwanted supply to be

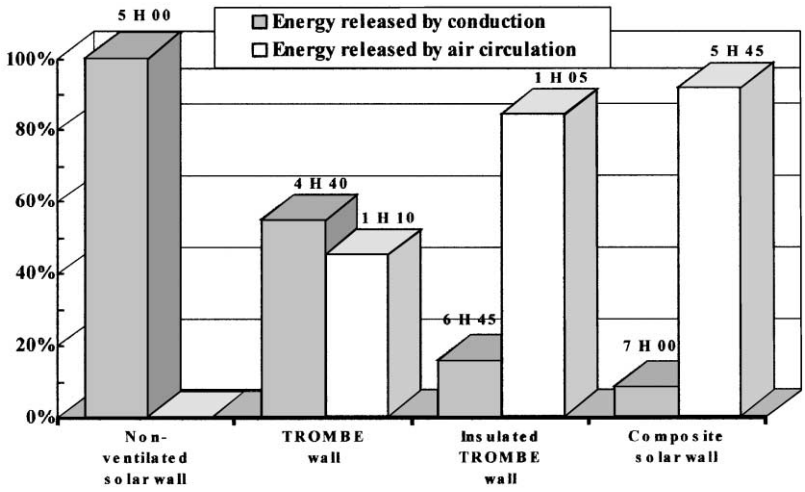

Fig. 16. Release mode and times.

divided by 2.6 in the summer. These results are valid whatever site is chosen for walls which are not equipped with solar shields.

The advantages of installing or not installing solar protection should be evaluated depending on the site and the type of solar wall.

6. Conclusion

This article has presented the principle and part of the results concerning validation of a simulation model of the thermal operation of solar walls.

This model, developed in a standard manner, has been validated using numerous experimental results obtained over a long period of monitoring (3 years) on a test cell under real operating conditions. It was then possible to use this model to study the effect of design parameters or new materials (important for the future development of solar walls) and to compare different types of solar walls. These results are essential elements for designers. They may be used to optimise the choice of one or other configuration depending on the environment (the site) and the function of the building (accommodation, individual houses, offices, etc.). These walls will, therefore, be able to participate in the best possible manner in improving the efficiency for collecting "free" energy and will no longer be a handicap for managing comfortable environments (particularly in the summer, to avoid overheating).

Acknowledgements

We would particularly like to thank Mr. Chantant, engineer at the C.E.A. at Cadarache, who initiated this research, for his participation in writing this article. We would also like to thank the Nord-Pas-de-Calais region for co-funding Mr. Zalewski's thesis work, in association with the C.E.A.

References

[1] Trombe F. Maisons solaires. Techniques de l'Ingénieur 3 C777, 1974.
[2] Ben Yedder R, Bilgen E. Natural convection and conduction in Trombe wall systems. International Journal of Heat and Mass Transfer 1991;34(4/5):1237.
[3] Detuncq B, Bilgen E. Etude expérimentale d'un capteur solaire du type Trombe et validation des relations théoriques. Note technique. Transactions of the C.S.M.E 1984;18(1):35–9.
[4] Smolec W, Thomas A. Theoretical and experimental investigations of heat transfer in a Trombe wall. Energy Conversion, Management 1993;34(5):385–400.
[5] Utzinger DM, Klein SA, Mitchell JW. The effect of air flow rate in collector–storage walls. Solar Energy 1980;25(4):511–9.
[6] Bilgen E. Composite wall storage–collector systems for passive utilization of solar energy in cold climates. Ecole Polytechnique, Génie mécanique, Montréal. ASME 1987;4.
[7] Zrikem Z, Bilgen E. Theoretical study of a composite Trombe–Michel wall solar collector system. Solar Energy 1987;39(5):409–19.
[8] Zalewski L. Etude thermique expérimentale et simulation numérique d'un mur solaire composite-Optimisation des performances énergétiques. Doctorat de l'université d'Artois, November 1996.
[9] Thery P, Kougbeadjo RA, Leclerq D. Mesure simultanée de flux et température. Journées Industrielles de la Société Physique, Toulouse, Mars 1980.
[10] Lassue S. Analyse des échanges radiatifs et convectifs à la surface d'une paroi opaque. Application à la commande optimale du système habitat. Thèse de doctorat, Lille, 1989.
[11] Lassue S, Guths S, Leclercq D, Duthoit B. Contribution to the experimental study of natural convection by heat flux measurement and anemometry using thermoelectric effects. Conference on experimental heat transfer, fluid mechanics and thermodynamics, Honolulu, HI, USA, October 1993.
[12] Zalewski L. Etude expérimentale des transferts thermiques dans la lame d'air ventilée d'un mur solaire. Concours jeunes chercheurs de l'AUGC — Clermont-Ferrand, Mai 1996.

[13] Zalewski L, Chantant M, Lassue S, Duthoit B. Experimental thermal study of a solar wall of composite type. Energy and Buildings 1997;25(1):7–18.
[14] Lassue S, Zalewski L, Defer D, Duthoit B, Chantant M. Mesures fluxmétriques et notion d'impédance thermique appliquées à la caractérisation d'une paroi de bâtiment soumise à des sollicitations naturelles. Materials and Structures 1996;29:219–25.
[15] Zalewski L, Lassue S, Duthoit B. Heat flux measurement applied to the study of thermal heat transfers in a composite solar wall. Congrès Latino-Américain en sciences thermiques — Florianopolis, Bresil, November 1996.
[16] Other L. Application des méthodes de la théorie des systèmes à la simulation de l'évolution des flux thermiques sur les faces d'entrée et de sortie d'une paroi multicouche. Thèse de 3ème cycle, Lille, 1996.
[17] Zalewski L, Lassue S, Duthoit B, Chantant M. Etude des transferts thermiques dans un mur solaire composite et validation d'un modèle de simulation numérique. Conférence Internationale Energie Solaire et Bâtiment, Lausanne, Octobre 1997.
[18] Kougbeadjo RA. Identification de la diffusivité thermique par traitement du transfert de chaleur à travers une paroi homogène en régimes impulsionnel et pseudo-aléatoire — Application des méthodes de corrélation en thermocinétique. Thèse de 3ème cycle, Lille, 1981.
[19] Juval-Lambert H. Programmation de la technique des plans factoriels à deux niveaux appliquée à la mesure des effets et à la modélisation. Rapport de stage de DESS, Marseille, 1993.
[20] Lebart L, Morineau A, Fenelon JP. Traitement des données statistiques. Paris: Dunod, 1982.